

SNS INJECTION AND EXTRACTION DEVICES*

D. Raparia[#]

for the Spallation Neutron Source Collaboration, USA.

INTRODUCTION

The Spallation Neutron Source (SNS) project is designed to reach an average beam power above 1.4 MW for pulsed neutron production [1, 2]. The accelerator system operates at a repetition rate of 60 Hz and average current of 1.4 mA. It consists of an H⁻ 1 GeV superconducting linac; a high energy beam transport (HEBT)[3] for diagnostics, transverse and longitudinal collimations, matching, energy correction and painting; and an accumulator ring compressing the 1GeV, 1 ms pulse to 650 ns for delivery onto target through a ring-target beam transport (RTBT)[4].

At such intensity and power, beam loss is critical issue mainly for two reasons; (1) to guarantee hands-on maintenance of the accelerator; (2) to protect components of the accelerator. The injection loss and subsequent beam loss due to all injection mechanisms has to be kept manageable. There are several injection loss mechanisms. These are: 1) the linac beam missing the stripping foil, 2) H⁰'s emerging from the foil, which is a function of the thickness of the foil, 3) H⁻'s emerging from the foil, which is calculated to be negligible, and 4) circulating beam loss due to Coulomb and nuclear scattering on the foil. Loss mechanism 1) is related to the stripping foil size and this loss should be kept to less than a few percent. This beam loss along with loss due to mechanism 3) is well known and a controlled dumping of the waste beam is planned [5]. Loss mechanism 4) is directly related to the thickness of the foil and the amount of circulating beam hitting it, which is proportional to the foil size [6]. The foil size is chosen such that it provides a compromise between mechanisms 1) and 4). The thickness of the foil is determined by mechanisms 2), 4) and the foil heating problem [7]. Present plans call for a carbon foil of size of 8 mm x 4 mm and a thickness of 300 mg/cm².

The size of the stripping foil is chosen such that a distribution tail of about 2% of the incoming linac beam misses the foil. This is a compromise between this loss and the loss due to Coulomb and nuclear scattering of the stored protons. For a 400-μg/cm² thick foil, about 0.82% and for a 300-μg/cm² foil about 2% of the incoming H⁻ ions will emerge as H⁰. The population of their quantum of H⁰ states is measured to be n-2.8, where n is the principal quantum number. The H⁰'s that emerge from the foil are converted to protons by a thick foil placed in their path. The downstream magnets will separate those protons from the circulating protons. The septum magnet downstream is to be combined function magnet and

together with the quadrupole placed downstream shapes the image of the dumped proton beam on to the 200 kW beam dump.

For 1 GeV injection, the stripped electrons from the incoming H⁻ beam have about one thousandth of the proton power and is 1 kW at 1 MW SNS, which is formidable electron power. It is essential to dump these electrons proper way to avoid electron cloud instability [16] and over heating of components.

INJECTION

Injection takes place in one of the near-dispersion-free straight section of the ring [8]. The process is controlled by a large, especially designed, fixed orbit bump. The fixed orbit bump is a chicane consisting of four dipole magnets in the long straight section between quadrupole doublets. The schematic plan view of the injection straight section is shown in Figure 1. Figure 2 show the layout of the injection section.

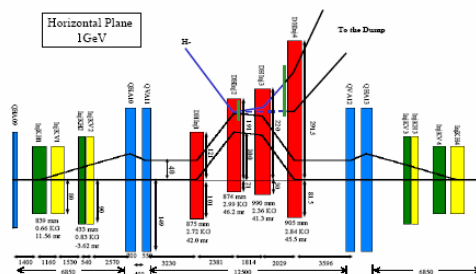


Figure 1: Injection schematics (horizontal layout).

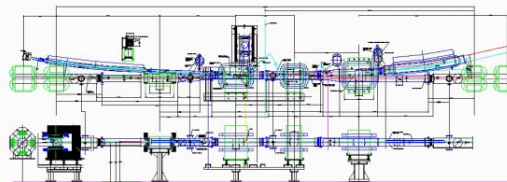


Figure 2: Layout of the injection region.

To facilitate the clean dumping of the H⁰ atoms excited by the stripping foil, injection takes place in the downstream fringe field of second of this chicane dipole. This dipole, which is a C-type magnet, has a central magnetic field of 3 kG. However the stripping foil is located at the edge of the magnet in a 2.5-kG field region. The magnetic field value is important because the electric field felt by the moving excited H⁰ is such that the principal quantum numbers of n=4 or less survive the field, whereas those of n=5 or higher strip immediately.

*SNS is managed by UT-Battelle, LLC, under contract DE-AC05-00OR22725 for the U. S. Department of Energy. SNS is a partnership of six national laboratories: Argonne, Brookhaven, Jefferson, Lawrence Berkeley, Los Alamos, and Oak Ridge

[#]raparia@bnl.gov

The spatially decreasing nature of the fringe field assures that the excited H⁰'s that are not stripped immediately will probably not be stripped at all because the field is decreasing, and hence the electric field felt by the H⁰'s will be too low. The third chicane magnet field is 2.4 KG which is lower than the field which the H⁻ are stripped. The uncontrolled loss by the Stark stripping of the excited H⁰'s is estimated to be on the order of 10⁻⁶ of the injected H⁻ beam. Even if the energy gap between the n=4 and n=5 states is completely miscalculated, the uncontrolled loss rate would be 10⁻⁵.

At the upstream end of the chicane, in the HEBT injection line, a 3 meter long septum magnet with a 2.03 KG field to bring the beam from the HEBT line to the foil, while avoiding the upstream quadrupole and the circulating beam. In front of the last chicane magnet relatively thick stripping foil is placed to strip the electrons of un-stripped H⁰ and H⁻ to protons. At the downstream of the last chicane magnet, there is a ~2-meter long septum magnet with a field of 5 kG to take the un-stripped H⁻ and H⁰ ions to the external injection dump. This septum is a combined function magnet to manipulate two beams originated from the un-stripped H⁻ and H⁰ ions. A water cooled carbon-carbon block at the lower surface of the vacuum chamber under the stripping foil to intercept the stripped electrons from the H⁻ injected beam. Two sets of kickers (pulsed dipoles), a set of four (4) for each plane, are used to create dynamic orbit bumps in order to paint the optimum phase space of the injected proton population. The kickers are located in the two shorter straight space of the straight section. The kicker magnets are programmable with time constant as fast as 200 μs.

The field quality requirement for the ring magnet is very stringent and limited 10⁻⁴ for the ring magnets with respect to the ring main dipole, and 10⁻³ for the transfer line magnets. Low carbon steel (1006) was used for all the SNS ring and transfer line magnets.

DC Magnets for Injection Region

There are six DC magnets for injection area; 3 meter long septum magnet in the HEBT; four chicane magnets to create closed 10 cm bump at the injection foil; and 2-meter long combined function septum magnet. Table I show their main parameters.

Table I: main parameters for injection area DC magnets.

	L (m)	G (cm)	B (kG)	Coil/pole	I (kA)
Inj. Sept.	3.0	6.8	2.03	2	2.8
CH #1	0.74	28.5	2.28	8	3.2
CH #2	0.70	24.8	3.00	14	2.168
CH#3	0.48	24.8	2.40	14	1.720
CH#4	0.67	24.1	2.95	14	2.025
D. Sept.	1.93	7.0	4.5	4	2.833

Injection Septum

A Three-meter long septum magnet is located at upstream end of the chicane in the HEBT which bring the beam from HEBT to the foil, while avoiding the upstream

quadrupole and circulating beam. A model of the magnet and picture of it is shown in Figure 3. Magnet is design to shield the fringe field from circulating beam.

Measurements of the magnet show that the integrated fringe field as seen by the circulating beam is less than 3 G-m.

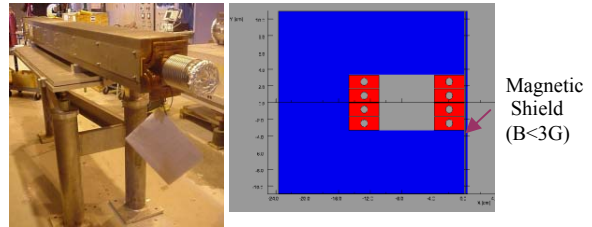


Figure 3: Photo and TASCADA model of the injection septum magnet.

Chicane #1

The first magnet in the chicane has relatively wider then the length. It was design with great care to reduce higher multipoles with the acceptable limit with help of so called z-bump (shims) and grooves in the magnet as shown in the Figure 4. To avoid mechanical interference with the injecting beam line, this magnet was designed so that circulating beam pass through this magnet about 4 mm horizontally off centered.

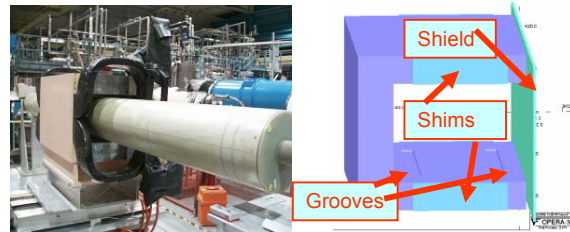


Figure 4: Model and photograph of chicane#1.

It took several iterations to optimize size of the z-bumps and length of the grooves to reduce the multipoles with in the acceptable limit. Table II shows the measurement results

Table II: multipoles for the Chicane #1.

Harmonics in Chicane #1 at various stages
 Estimated Integral harmonics at 3500A at X=10 mm, and 80 mm reference radius
 These harmonics are estimated using feed down from the center position measurements
 Measured data are centered using measuring coil position determined from survey

ITF (Tm/kA)	SNGCH102.104				SNGCH105.104				SNGCH108.103				SNGCH114.103						
	As-built	End Plates removed	End Plates and strips removed	2nd Zbumps	As-built	End Plates removed	End Plates and strips removed	2nd Zbumps	As-built	End Plates removed	End Plates and strips removed	2nd Zbumps	As-built	End Plates removed	End Plates and strips removed	2nd Zbumps			
b1	0.07571	0.07378	0.07329	0.07456	--	--	--	--	a1	6.4	6.5	6.5	6.6	a1	6.4	6.5	6.5	6.6	
b2	-45.3	-21.4	-45.9	-5.0	b2	-0.7	-0.7	-0.7	-0.7	a2	-0.7	-0.7	-0.7	-0.7	a2	-0.7	-0.7	-0.7	-0.7
b3	5.8	6.1	1.1	3.9	b3	0.4	0.4	0.4	0.4	a3	0.4	0.4	0.4	0.4	a3	0.4	0.4	0.4	0.4
b4	-12.6	-13.9	0.5	-5.5	b4	-0.1	-0.1	-0.1	-0.1	a4	-0.1	-0.1	-0.1	-0.1	a4	-0.1	-0.1	-0.1	-0.1
b5	0.0	-0.1	0.6	1.3	b5	0.0	0.0	0.0	0.0	a5	0.0	0.0	0.0	0.0	a5	0.0	0.0	0.0	0.0
b6	0.2	0.4	-1.0	-1.8	b6	0.0	0.0	0.0	0.0	a6	0.0	0.0	0.0	0.0	a6	0.0	0.0	0.0	0.0
b7	-0.2	-0.2	0.2	0.1	b7	0.0	0.0	0.0	0.0	a7	0.0	0.0	0.0	0.0	a7	0.0	0.0	0.0	0.0
b8	0.3	0.4	-0.3	-0.1	b8	0.0	0.0	0.0	0.0	a8	0.0	0.0	0.0	0.0	a8	0.0	0.0	0.0	0.0
b9	0.3	0.3	0.1	0.0	b9	0.0	0.0	0.0	0.0	a9	0.0	0.0	0.0	0.0	a9	0.0	0.0	0.0	0.0
b10	-0.3	-0.3	-0.1	0.0	b10	0.0	0.0	0.0	0.0	a10	0.0	0.0	0.0	0.0	a10	0.0	0.0	0.0	0.0
b11	0.0	0.0	0.0	0.0	b11	0.0	0.0	0.0	0.0	a11	0.0	0.0	0.0	0.0	a11	0.0	0.0	0.0	0.0
b12	0.0	0.0	0.0	0.0	b12	0.0	0.0	0.0	0.0	a12	0.0	0.0	0.0	0.0	a12	0.0	0.0	0.0	0.0
b13	0.0	0.0	0.0	0.0	b13	0.0	0.0	0.0	0.0	a13	0.0	0.0	0.0	0.0	a13	0.0	0.0	0.0	0.0
b14	0.0	0.0	0.0	0.0	b14	0.0	0.0	0.0	0.0	a14	0.0	0.0	0.0	0.0	a14	0.0	0.0	0.0	0.0

Chicane #2 and #3

These two magnets are very special and designed with grate care. These magnet has following constrains: (1) field strength of chicane #2 should be lower than 3 kG to minimize the H⁻ stripping and field at the foil should be 2.5 kG; (2) filed strength of chicane #3 should be more than 2.4 kG and lower than 3.0 kG to tripped H⁰ excited state higher than n=5; (3) filed angle $\tan^{-1}(B_z/B_y) \gg 65$ mrad to stop stripped electrons to spiral back to foil; (4) the filed integral from $-\infty$ to foil should be 237.6 kG-cm and foil to $+\infty$ should be 261.4 kG-cm; and (5) multipoles of combined filed should be lower than 5×10^{-3} .

These constrains were achieved with special design of poles in these magnets. To satisfy the field angle requirements lower pole of chicane #2 was wider than the upper pole and to satisfy the multipoles requirements for both magnets combine, chicane #3 poles were reversed. Figure 5 shows the photograph of chicane #2 & #3. These magnet were measure with rotating coil of radius 40.8 mm and length 4.75 m and results are summarized in Table III



Figure 5: Photograph of chicane #2 and #3.

Table III: multipoles for the Chicane #2 and #3.

Integral Field Quality Measurements in Chicane #2 & #3
Measurements with a 40.8 mm radius, 4.75 m long coil
Harmonics expressed in 10⁻⁴ "units" at 80 mm radius

Harmonic	Chicane #2 (2154.8 A)	Chicane #3 (1732.0 A)	Chicane #2 (2154.7 A) + Chicane #3 (1733.2 A)	Chicane #2 + #3 (2154.7 A/1733.2 A) Normalized to 17D120 field
$\int B \cdot dl$ (T.m)	0.3006	0.2016	0.5012	1.106
b_1	-1.8	-4.1	-1.9	-0.9
b_2	-8.2	-9.4	-9.2	-4.2
b_3	1.2	0.9	1.3	0.6
b_4	0.0	-0.4	-0.1	-0.1
b_5	0.5	-0.7	0.0	0.0
b_6	-0.9	0.0	-0.6	-0.3
a_1	116.0	-158.2	6.2	2.8
a_2	-8.0	9.6	-0.9	-0.4
a_3	8.0	-11.3	0.3	0.1
a_4	-0.5	0.4	-0.1	-0.1
a_5	1.5	-1.3	0.0	0.0
a_6	0.1	-0.3	0.0	0.0

Filed angle at foil and filed were measured with a single LPT-141 Hall probe. Measurements were repeated after flipping the probe 180 degrees to minimize errors due to Hall element position and orientation uncertainties. Estimated over all error due to probe calibration (0.1%), probe position (0.1 mm), prove orientation (< 2mrad) is

less than 3 mrad. The measured filed angel is 214 mrad whereas calculated filed angle is 208 mrad. . Measured filed integral from $-\infty$ to foil is 237.95 kG-cm and foil to $+\infty$ is 261.74 kG-cm at the mid plane. These magnets were so well designed that meets all the requirements with any additional shimming etc. The stripped electrons were track with the measured field to locate the electron catcher [9].

Chicane #4

This is the last magnet in the chicane. It accommodates all three ion trajectories, namely circulating proton, protons stripped from H⁰ and proton stripped from H⁻ and has relatively large width. It was design with grate care to reduce higher multipoles for circulating beam within the acceptable limit with help of z-bump. Figure 6 shows the photograph of the magnet.



Figure 6: Photograph of chicane #4.

It took four iterations of z-bump and a horizontal magnet shift of 6 cm to reduce multipoles within acceptable limit. The field quality measurements were taken using a long flip coil at various locations within the beam area of radius 5 cm (300π mm mrad) and 8 cm (480π mm mrad). The measured field is flat to 5 parts in 10,000 (5 units) everywhere within the 5 cm radius and is flat to 7.5 units within the 8 cm radius.

Injection Dump Magnet

This magnet is a 2 m long combined function magnet. It carries both protons trajectory (stripped from H⁰ and H⁻) and focuses them onto injection beam dump. The gradient is about 1 T/m. Since the magnification of beam from charge exchange foil to dump is about 100, therefore this magnet is very sensitive errors and designed and measure with very carefully. Figure 7 shows the photograph of the magnet.

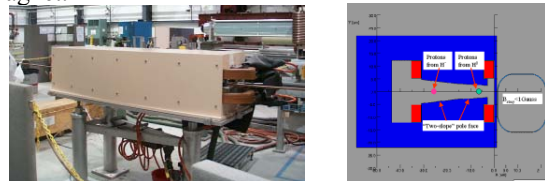


Figure 7: Photograph and model of the injection dump gradient magnet.

To avoid mechanical interference with the circulating beam pipe, magnet was rotated ~ 1.5 degrees about it center. It took four iterations of z-bump to get the correct ratio of integrated field for proton stripped from H⁰ and

proton stripped from H⁻. Figure 8 shows the measurement results.

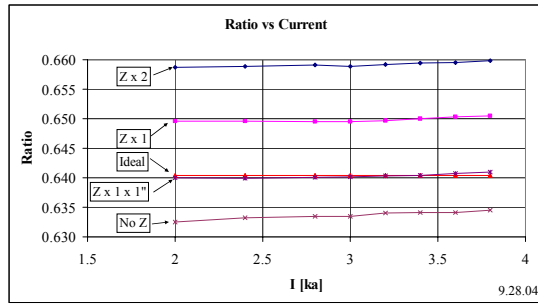


Figure 8: Measurement result showing ratio of integrated filed for proton generated from H⁰ and H⁻.

Dynamic Orbit Bump Magnets for Injection Area

The function of the dynamic orbit bump is to create additional orbit bump on top of the DC chicane of the injection. The dynamic bump shall be fast enough to be able to paint the injected beam density in the phase space in the way minimizes the space charge effects and to minimize a possibility of any transverse instabilities and optimize current density at the target. Power supplies are programmable and have time constants as fast as 200 μs. The dynamic bump consists of four, two short and two long magnets in each of the x y direction located short free spaces of the injection straight section. Table IV shows the specification for dynamic bump magnets. Figure 8 shows the photograph of long dynamic bump magnets.

Table IV: Specification for dynamic bump magnets

	Long	Short
Number	4	4
Core length	64 cm	21 cm
Aperture	19.55 x 22.58 cm	21.55x24.48cm
# of Turns	10	12
Max. Current	1230 A	1400A
Max. Field	0.079 T	0.1 T
Ceramic Vac. Chamber ID	16 cm	18 cm



Figure 8: Long Injection dynamic bum magnets with Beam Pipe and Bellow.

EXTRACTION

The accumulated beam in the SNS ring forms a single 590 ns long bunch with gap of 250 ns. The extraction system consists of 14 fast kickers and a single Lambertson septum magnet. Extraction is a two step process: kick the beam (13.6 mrad) vertically down with the fast kickers into the Lambertson septum magnet, and then use the septum magnet to deflect the beam horizontally (16.8 degrees) [10]. Ring extraction layout and orbit is shown in Figure 9.

In most machines, the extraction region has a high radio activation level resulting from accidental beam loss caused by missteering and kicker malfunction. The SNS ring extraction system is designed to accept the fully painted beam without loss even when one of 14 kickers fails. The acceptance of the extraction channel is 400 π mm mrad, as compare to the ring acceptance of 480 π mm mrad. To achieve a fractional beam loss below 10⁻⁶ at the extraction channel under normal operating conditions, the beam is collimated for an extra 20 turns after accumulation.

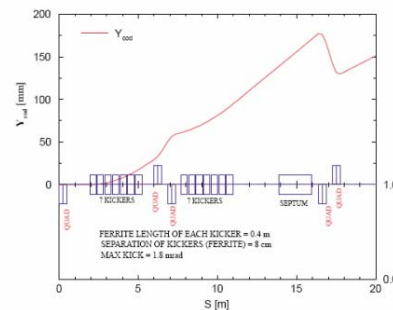


Figure 9: Ring extraction layout and orbit. The beam is kick vertically by 14 kickers and extracted horizontally by a Lambertson septum magnet.

Lambertson Magnet

In order to maximize the vertical displacement of the extracted beam at the entrance of the septum magnet was placed as far as possible from the kickers. The locations of the septum magnet in conjunction with the angle of bend and beam size, define following set of parameters for the septum magnet: effective length = 2.44 m; magnetic filed = 0.68 T; bend angle = 16.8 degrees; gap (extracted beam) = 16.9cm; aperture for circulating beam = 17.5 cm, septum thickness = 1.0 cm. Extracted beam must be at target elevation and parallel to the RTBT. The Lambertson magnet war rotated about 2.5 degrees to oppose the vertical kick from the kickers. Residual vertical angle will be corrected with shift the first quadrupole in the RTBT. [11-13]

To reduce the magnetic field at the circulating beam region extended shielding was provided, circulating beam pipe was made with 1010 steel, and about 1 mm copper shielding was place between pipe and the magnet iron.

The integrated field for the circulating field was measured with a 40 mm radius, 4.75 meter long rotating

coil at three vertical positions -36.3 mm, +0.6 mm and +37.6 mm from the vertical center of the aperture. The coil was slightly tilted in the vertical plane to match the tilt of the beam tube. To reduce the multipoles we have to add extra shielding in the both ends. As shown in figure 10.

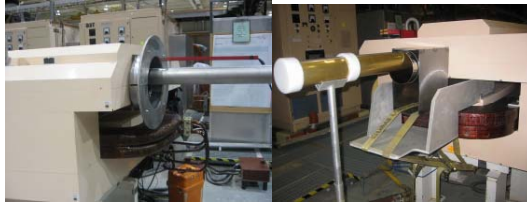


Figure 10: Magnetic shielding downstream (left) and upstream (right).

The measurement results are shown in Figure 11. All the multipoles are below 10^{-4} except dipole component which is about 30 G-m. The maximum close orbit distortion due to this dipole component is about 1.2 mm and maximum corrector strength is only 23% of the corrector strength available.

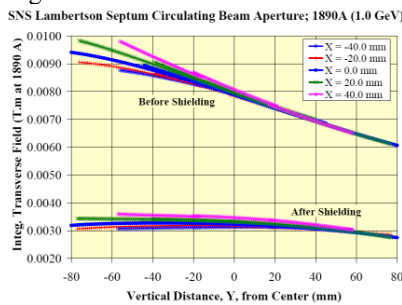


Figure 11: measurement result for circulating beam pipe before and after added extra shielding in both ends as shown in figure 10.

Magnetic measurements for the extracted beam were made by flip coil on a (x, y) grid with x=(9-62.2 mm, -31.1 mm, 0.0 mm, 31.1 mm, +62.2mm) and y=(-65.2 mm, -32.6 mm, 0.0 mm, +32.6 mm, +65.2 mm) For the uppermost and the lowermost positions, the outmost horizontal positions could not be measured due to difficulties in flipping the coil. So there are total of 21 (x, y) combinations that were measured. The measurement result is shown in Figure 12.

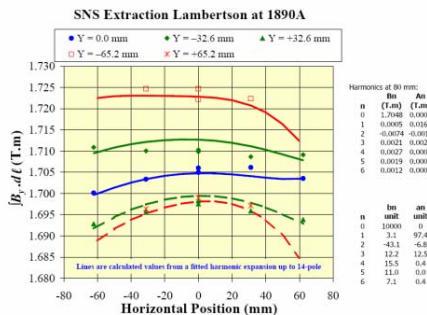


Figure 12: Magnetic measurement results for the extracted beam.

Extraction Kicker Magnets

Fourteen window frame ferrite magnets were assembled in two modules [14]. Seven kickers magnets in one assembly are located upstream of a quadrupole-doublet, and seven magnets in another assembly are located downstream of the quadrupole-doublet. The inner surface of the kickers were coated with TiN [15] to reduce the secondary electron yield. The location of each of the kicker was optimized to minimize the required voltage. The length of the kicker was optimized to reduce the ratio of inductance to kick. Each kicker will be excited by a pulse forming network (PFN) operated at 60 Hz with a flat top of 750 ns and a rise time of 200 ns.

The fourteen kickers were designed with various apertures and length to minimize losses and optimize the impedance. To simplify the kicker design and ease of installation and maintenance, the 14 magnets are grouped in 6 different types. Figure 13 shows the extraction kicker assembly.



Figure 13: Extraction kicker assembly.

Before final installation, 3 of the kicker magnets in the downstream kicker were assembled and powered to 35 KV as in operating condition to check its waveform and performance.

ACKNOWLEDGEMENT

We are indebted to the SNS team and our collaborators for their devotion and contributions.

REFERENCES

- [1] T. Mason, these proceedings
- [2] J. Wei, these proceedings
- [3] D. Raparia, et al, PAC 1997, pp 162
- [4] D. Raparia, et al, PAC 1999, pp 1297
- [5] D. Raparia, et al, PAC 2003, pp 3418.
- [6] D. Raparia, et al, PAC 2001, pp 3260
- [7] J. Beebe-Wang, et al, PAC 2001, pp 1508.
- [8] J. Wei, et al, PAC 2001, pp 2560.
- [9] Y. Y. Lee, et al, these proceedings
- [10] N. Tsoupas, et al, EPAC 2000, pp 2270
- [11] J. Rank, et al, PAC 2003, pp 2150
- [12] N. Tsoupas, et al, PAC 2001, pp 3245
- [13] J. Rank, et al, these proceedings
- [14] C. Pai, et al, these proceedings
- [15] H. C. Hseuh, et al, these proceedings
- [16] L. Wang, et al, these proceedings